Cancer Chemother Pharmacol (2011) 68:777–786
DOI 10.1007/s00280-010-1517-4

ORIGINAL ARTICLE

Pharmacokinetics, pharmacodynamics and metabolism of the dimeric pyrrolobenzodiazepine SJG-136 in rats

Joel M. Reid · Sarah A. Buhrow · Mary J. Kuffel · Lee Jia · Victoria J. Spanswick · John A. Hartley · David E. Thurston · Joseph E. Tomaszewski · Matthew M. Ames

Received: 26 March 2010 / Accepted: 29 October 2010 / Published online: 28 December 2010

Abstract
Purpose The dimeric pyrrolobenzodiazepine SJG-136 (NSC 694501, SG2000) has potent in vitro antiproliferative activity and in vivo antitumor activity associated with binding in the minor groove of DNA and formation of covalent interstrand DNA cross-links. The pharmacokinetics and in vitro metabolism of SJG-136 and as well as the feasibility of using the Comet assay to measure in vivo interstrand DNA cross-links, was assessed in the rat.
Methods SJG-136 pharmacokinetics and pharmacodynamics were characterized in rats following single-dose administration of 15 and 50 μg/kg or multiple-dose administration of 25 μg/kg/day for 5 days. DNA damage was measured in peripheral blood mononuclear cells using the Comet assay. SJG-136 oxidative metabolism was characterized in rat liver microsomes.
Results SJG-136 half-life, clearance and volume of distribution values were 9 min, 190 ml/min/m^2, and 1780 ml/m^2, respectively. SJG-136 did not accumulate in plasma during treatment with 25 μg/kg/day for 5 days. Treatment with SJG-136 produced the anticipated DNA interstrand cross-links, as well as DNA strand breaks, in rat PBMCs. Oxidative metabolism of SJG-136 in rat liver microsomes was catalyzed by CYP3A isoforms and produced a previously unreported monomeric metabolite.
Conclusions Plasma concentrations of SJG-136 associated with pharmacological activity and in vitro antiproliferative activity were achieved with doses that were tolerated by rats. CYP3A isoforms are the predominant P450s catalyzing SJG-136 metabolism. The comet assay detects DNA damage in PBMCs from rats treated with SJG-136 and is being used in clinical trials to monitor in vivo lesions produced by SJG-136.

Keywords Pyrrolobenzodiazepine dimer · DNA damage · Pharmacokinetics · Metabolism · Pharmacodynamics · Comet assay

Abbreviations

CYP	Cytochrome P450
PBMC	Peripheral blood mononuclear cells
Comet	Single cell gel electrophoresis

SJG-136 is owned by Spirogen Ltd in which J. A. Hartley and D. E. Thurston have equity interests.

J. M. Reid · S. A. Buhrow · M. J. Kuffel · M. M. Ames (✉)
Division of Oncology Research, Gonda 19-363, Mayo Clinic, 200 First Street SW, Rochester, MN 55905, USA
e-mail: ames.matthew@mayo.edu

L. Jia · J. E. Tomaszewski
DTP, National Cancer Institute, Bethesda, MD, USA

V. J. Spanswick · J. A. Hartley
Cancer Research UK Drug-DNA Interactions Research Group, UCL Cancer Institute, Paul O'Gorman Building, University College London, London, UK

D. E. Thurston
School of Pharmacy, University of London, London, UK

Introduction

The dimeric pyrrolobenzodiazepine SJG-136 (8,8′-[{(propane-1,3-diyl)dioxy}-bis[(11aS)-7-methoxy-2-methylidene-1,2,3,11a-tetrahydro-5H-pyrrolo{2,1-c}[1,4]benzodiazepin-5-one], NSC 694501, Fig. 1) is a sequence-selective, bifunctional DNA-alkylating agent with potent in vitro cytotoxicity and in vivo antitumor activity [1, 2]. Naturally occurring

pyrrolobenzodiazepine monomers such as anthramycin, tomaymycin, and DC-81 exert their cytotoxic effect by covalent binding to the N2 of guanines in the minor groove of DNA via their C11 position [3]. The first bifunctional analog in this series, DSB-120 (Fig. 1), was synthesized by connecting two DC-81 monomers via their C8 positions with a 1,3-propanediyldioxy ether linkage [4]. DSB-120 had potent in vitro cytotoxicity but poor in vivo antitumor activity, thought to be mainly due to inactivation by reaction with glutathione found in biological fluids and hemolysed blood [5, 6]. SJG-136, which has methylene moieties at the C2/C2′-positions, was subsequently designed to be less electrophilic at the N10-C11/N10′-C11′ functionalities and thus less reactive toward glutathione [1, 2]. This analog maintained sequence-specific cross-linking activity and potent in vitro cytotoxicity and possessed significant in vivo antitumor activity [7, 8]. Furthermore, SJG-136 exhibited three to fourfold greater in vitro cytotoxicity toward malignant B-cells and T-cells from patients with B-cell chronic lymphocytic leukemia when compared to normal B- and T-PBMCs [9]. As with DSB-120, the potent antiproliferative activity was thought to be associated with binding in the minor groove of DNA and formation of interstrand cross-links through reaction of the N^{10}-C^{11} and $N^{10'}$-$C^{11'}$ imine moieties and the N2 groups of guanine bases on opposite DNA strands [10]. More recently, it has been shown that SJG-136 can form both interstrand and intrastrand cross-links with two to four DNA base pairs between participating guanines, and also adducts resulting from mono-alkylation at sequences containing only one PBD-binding site and devoid of a second suitably positioned guanine [11]. However, the Pu-GATC-Py interstrand cross-link is still thought to be the major lesion in terms of the cytotoxicity and antitumor activity of SJG-136.

SJG-136 exerted potent, differential inhibition in the NCI Developmental Therapeutics Program's in vitro 60 cell line panel with an average GI_{50} of 7.4 nM (range, 0.14–320 nM) [8]. According to the NCI's COMPARE algorithm, the activity profile did not align with cluster patterns associated with other DNA-binding agents and was thus consistent with a distinct mechanism of action. [8]. Cell killing by SJG-136 in B-CLL cells was shown to be mediated by caspase 9 signaling, and to be dependent on caspase 3 activation but independent of p53 status [9].

SJG-136 exhibited broad spectrum in vivo antitumor activity in both hollow fiber and human tumor xenograft models using multiple treatment regimens over a relatively wide dose range [7]. Potent in vivo antitumor activity was observed across a broad range of tumor models utilizing multiple schedules with doses as low as 0.2 mg/kg per dose still active. Significant growth delays were observed in human tumor xenograft models following qdx5 and q4dx3 schedules, with better efficacy produced by the qdx5 schedule [7]. Crucially, evaluation in ovarian cancer xenograft models demonstrated potent in vivo activity against both cisplatin-sensitive and cisplatin-resistant tumors, a property thought to be due to the non-distortive DNA adduct formed by SJG-136 [8].

SJG-136 has recently completed Phase I clinical trials in the united Kingdom [12] and in the United States [13, 14], and is about to enter Phase II clinical investigation on the basis of the observed examples of partial responses and stable disease, particularly with dose schedules utilizing daily administration for 3 or 5 days every 3 weeks [14].

Preliminary pharmacokinetic investigations with DSB-120 and SJG-136 were performed in mice to measure achievable peak plasma concentrations and to characterize drug elimination. After a single 5 mg/kg i.v. dose of DSB-120, the peak plasma concentration was 47 μM with an elimination half-life value of 38 min [6]. After a single 0.2 mg/kg i.p. dose of SJG-136, the peak plasma concentration and half-life values were 336 nM and 59 min, respectively [15]. The metabolism and pharmacokinetics of SJG-136 in rats have not been previously reported. We now report these results along with the pharmacodynamic effects of SJG-136 with respect to the DNA lesions formed

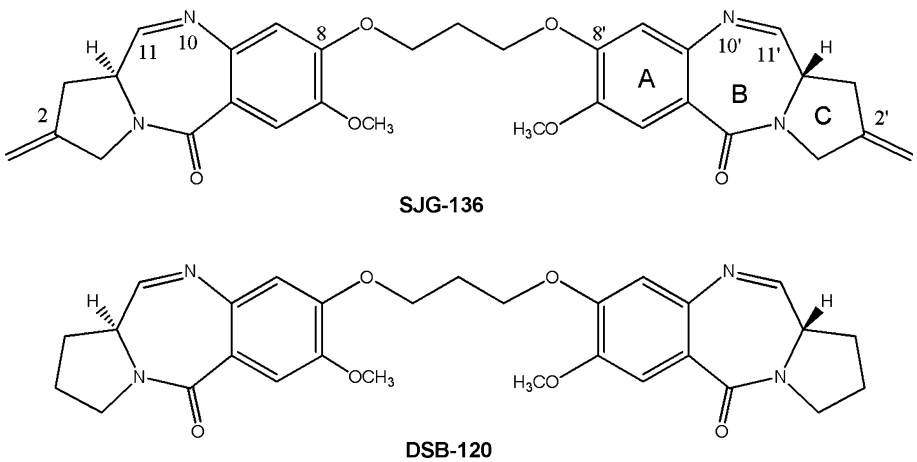

Fig. 1 Chemical structures of SJG-136 and DSB-120 (internal standard)

in PBMCs as measured by the Single Cell Gel Electrophoresis (Comet) assay.

Materials and methods

Reagents and materials

SJG-136 (8,8′-[{(propane-1,3-diyl)dioxy}-bis[(11aS)-7-methoxy-2-methylidene-1,2,3,11a-tetrahydro-5H-pyrrolo{2,1-c}[1, 4]benzodiazepin-5-one], MW 556) and DSB-120 (Fig. 1) with purity >95% determined by HPLC analysis were provided by the National Cancer Institute, Pharmaceutical Resources Branch, Division of Cancer Treatment (Bethesda, MD, USA). HPLC-grade acetonitrile, methanol, and water were purchased from EM Science (Gibbstown, NJ, USA). Formic acid (minimum 95%), citrate–phosphate dextrose solution, human serum albumin (fatty acid free and gamma-globulin free from fraction V; 96–99%), human α_1-acid glycoprotein (purified from Cohn fraction VI; 99%), anhydrous monobasic potassium phosphate, (minimum 99.0%) and *N,N*-dimethyl-acetamide (99+%) were purchased from Sigma Chemical Company (St. Louis, MO, USA). Heparin sodium (1,000 units/ml) was purchased from American Pharmaceutical Partners, Inc. (Los Angeles, CA, USA). Potassium hydroxide (Curtin Matheson Scientific, Inc., Houston, Texas, USA) and 0.9% sodium chloride solution (Baxter Healthcare Corporation, Deerfield, IL, USA) were purchased from commercial sources. Buffer solutions were prepared with deionized and distilled water.

Drug-free human plasma was obtained from healthy volunteers and frozen at −20°C. Rat and mouse whole blood was collected using 10% heparin in citrate–phosphate dextrose solution as an anticoagulant. The plasma was separated by centrifugation (10,000 rpm, 3 min, 4°C) and stored at −20°C for later use.

LC/MS/MS instrumentation

The LC/MS/MS system consisted of a Shimadzu liquid chromatograph (Wood Dale, IL, USA) with two LC-10ADvp pumps (flow rate 0.2 ml/min), and a SIL-10ADvp autoinjector (injection volume 20 µl) coupled to a triple quadrupole Quattro Micro mass spectrometer (Micromass, UK) fitted with an electrospray ionization probe in positive mode. SJG-136 detection was accomplished by MS/MS using the parent ion m/z 557.0 ($M + H^+$), a daughter ion m/z 476.0, with dwell 0.2 s, cone 40 volts and collision energy 30 eV. Internal standard (DSB-120) was detected by MS/MS using the parent ion m/z 533.20 ($M + H^+$), a daughter ion m/z 247.0, with dwell 0.2 s, cone 40 volts and collision energy 45 eV. The source temperature, desolvation temperature, cone gas flow and desolvation gas flow were 100°C, 120°C, 100 l/h and 250 l/h, respectively. MS data were collected for 5 min after sample injection. Spectra and chromatograms for SJG-136 and DSB-120 were processed using the Micromass software MassLynx v3.5. Metabolite detection was accomplished by MS scan scanning a start mass of m/z 50 to an end mass of m/z 700.

Chromatographic conditions

Separation of SJG-136 and DSB-120 was achieved using a Haipeek Clipeus C18 pre-column (20 × 2.1 mm i.d., 5 µm; Chrom Tech, Apple Valley, MN, USA) with a Genesis Lightning C18 analytical column (10 cm × 2.1 mm, 120Å, 4 µm; Jones Chromatography, Lakewood, CO, USA). The mobile phase consisted of water/acetonitrile (40:60, v/v) containing 0.1% formic acid and delivered at a flow rate of 0.2 ml/min. After sample injection, the column effluent was diverted to waste for 1 min, after which time the flow was switched to the mass spectrometer. After a 4-min run, the column was flushed with acetonitrile containing 0.1% formic acid for 1 min and equilibrated with water/acetonitrile (40:60, v/v) containing 0.1% formic acid for 3 min before the next injection.

Sample preparation

Stock solutions of SJG-136 and DSB-120 (1.0 mg/ml) were prepared in acetonitrile (SJG-136) and absolute ethanol (DSB-120) and stored at −20°C in silanized amber glass vials. Working standard solutions were prepared daily from the 1.0 mg/ml stock solutions using ice-cold acetonitrile. Plasma standards containing SJG-136 (0.78–100 ng/ml) and DSB-120 (50 ng/ml) were prepared by adding aliquots of the working standard solution to plasma (200 µl) measured into 12 × 75 mm glass tubes. Samples were kept on ice during the sample preparation procedure. SJG-136 and DSB-120 were isolated from plasma using solid phase extraction (SPE) with BondElute C8 (100 mg, 1 ml) cartridges (Varian, Harbor City, CA, USA). The SPE columns were pre-rinsed with methanol (2 × 1 ml) and KH_2PO_4 pH 6.0 (2 × 1 ml), loaded with plasma samples diluted with an equivalent volume of KH_2PO_4, pH 6.0 (200 µl), rinsed with KH_2PO_4 pH 6.0 (1 × 1 ml) and water (2 × 1 ml), dried for 5 min, and eluted with methanol (2 × 1 ml). Extracts were concentrated to dryness using a slow stream of nitrogen and finally reconstituted with 50:50 methanol:water (100 µl).

Drug formulation

SJG-136 (final concentration, 1 mg/ml, 1.8 mM) was dissolved in dimethylacetamide (DMA). The i.v. solution was prepared by mixing 0.06 ml of this drug solution with

0.09 ml DMA and 2.85 ml normal saline solution to achieve a final drug concentration of 36 μM.

Drug administration and specimen collection

Male Fisher CDF rats with surgically implanted jugular vein catheters were purchased from Charles River Laboratories (Wilmington, MA, USA). The intravenous dose of SJG-136 was administered via the catheter to rats lightly anaesthetized under methoxyflurane vapors. Blood samples (1.0 ml) were collected from the retroorbital sinus into silanized 2.0-ml microcentrifuge tubes containing 150 μl heparin solution per ml of whole blood. For the single-dose pharmacokinetic studies, blood samples (3–4 samples per rat) were collected before drug administration and 2, 5, 15, and 30 min, 1, 2, 4, 8, and 24 h after drug administration. Plasma was separated by centrifugation (10,000 rpm × 3 min), transferred to microcentrifuge tubes and then immediately frozen. For the multiple-dose pharmacokinetic study, blood samples were collected 30 min after treatment on Day 1 and Day 5.

To measure DNA damage using the Comet assay, blood samples were collected prior to drug administration and 1, 4, and 24 h after drug administration. PBMCs were isolated from these samples by centrifugation through a Ficoll-Hypaque density gradient. After washing with RPMI cell culture medium and re-suspension in RPMI medium containing 20% fetal calf serum and 10% DMSO, the cells were placed in cryovials, immediately frozen and stored at −80°C until analysis.

Comet assay for DNA damage

The details of the Single Cell Gel Electrophoresis (Comet) assay used to measure DNA interstrand cross-links in rat PBMCs following treatment with 15 and 50 μg/kg doses of SJG-136 are described in detail elsewhere [16]. All procedures were carried out on ice and under subdued lighting, and chemicals used were obtained from Sigma Chemical Company (Poole, UK) unless otherwise stated. Immediately before analysis cells were irradiated (10 Gy) in order to deliver a fixed number of random DNA strand breaks. After embedding cells in 1% agarose on a pre-coated microscope slide, they were lysed for 1 h in lysis buffer (100 mM disodium EDTA, 2.5 M NaCl, 10 mM Tris–HCl pH 10.5) containing 1% Triton X-100 added immediately before analysis, and then washed every 15 min in distilled water for 1 h. Slides were then incubated in alkali buffer (50 mM NaOH, 1 mM disodium EDTA, pH12.5) for 45 min followed by electrophoresis in the same buffer for 25 min at 18 V (0.6 V/cm), 250 mA. The slides were finally rinsed in neutralizing buffer (0.5 M Tris–HCl, pH 7.5) and then in saline.

After drying, the slides were stained with propidium iodide (2.5 μg/ml) for 30 min and then rinsed in distilled water. Images were visualized using a NIKON inverted microscope fitted with a high-pressure mercury light source, a 510–560-nm excitation filter and 590-nm barrier filter at ×20 magnification. Images were captured using an on-line CCD camera and analyzed using Komet Analysis software (Kinetic Imaging, Liverpool, UK). For each duplicate slide, 25 cells were analyzed. The tail moment for each image was calculated using the Komet Analysis software as the product of the percentage DNA in the comet tail and the distance between the means of the head and tail distributions, based on the definition of Olive et al. 1990 [17]. Cross-linking was expressed as percentage decrease in tail moment compared to irradiated controls according to the formula:

$$\%\,\text{decrease in tail moment} = \left[1 - \left(\frac{\text{TMdi} - \text{TMcu}}{\text{TMci} - \text{TMcu}}\right)\right] \times 100$$

where

TMdi = tail moment of drug-treated irradiated sample
TMcu = tail moment of untreated, unirradiated control
TMci = tail moment of untreated, irradiated control.

The following alternative Comet assay method was used to measure strand breaks in the single- and multiple-dose studies and to measure cross-links in the multiple-dose study employing a kit purchased from Trevigen (Gaithersburg, MD, USA). After embedding cells in 1% agarose on a pre-coated microscope slide, they were lysed for 2 h at 4°C in cold lysis buffer (100 mM EDTA, 2.5 M NaCl, 10 mM Tris–HCl, 1% sodium lauryl sarcosinate, 1% Triton X-100, pH 10 containing 10% DMSO). Slides were then incubated in alkaline solution (300 mM NaOH, 1 mM EDTA, pH > 13) for 1 h at room temperature followed by electrophoresis in the same buffer for 30 min at 1 V/cm, 300 mA. The slides were finally rinsed in distilled water and immersed in 70% ethanol for 5 min.

After drying, the slides were stained with dilute SYBR Green and allowed to dry overnight. Images were visualized using an Axioplan microscope (excitation/emission, 494 nm/521 nm) with a 0.63-adaptor, 40× lens, FITC filter and a 1300 × 1030 scanned resolution setting. Images were acquired using a KS400 imaging program with an exposure of 2,000–5,000. Image analysis was performed using a modification of the public domain image analysis program NIH Image [18]. Two slides were prepared and analyzed for each lymphocyte sample. Twenty-five images per slide were acquired for the positive (2 Gy exposure) and negative (no treatment) controls. Fifty images per slide were acquired from the samples collected after treatment with SJG-136. Cross-linking was expressed as percentage decrease in tail moment compared to irradiated controls calculated by the formula described above.

In vitro metabolism

Rat liver microsomes from untreated rats, and rats treated with intraperitoneal dexamethasone (300 mg/kg/day × 3), phenobarbital (80 mg/kg/day × 3) or 3-methylcholanthrene (20 mg/kg/day × 3) to induce cytochromes P450 were isolated by differential centrifugation of liver homogenates. Microsome suspensions of the B-lymphoblastoid cell line AHH-1 TK +/− expressing cDNA constructs for human CYP3A4, and the bacculovirus-insect cell line expressing cDNA constructs for rat CYP3A1 and CYP3A2 were obtained from Gentest Corporation (Woburn, MA, USA). Microsomes from cells with the vector alone and from cells without the vector were used as controls. Microsomal incubations were prepared in potassium phosphate buffer (100 mM) adjusted to pH 7.4 and incubated in amber glass vials maintained at 37°C in a shaker bath. Each incubation mixture (0.1–0.5 ml) contained SJG-136 (10 μM), NADPH (1.0 mM), magnesium chloride (5 mM) and rat liver microsomes (1 mg/ml protein) or individual recombinant P450 (50 pmol/ml). Identical incubations with active microsomes in which NADPH was omitted served as controls. After pre-incubation of the microsomes with the reaction buffer (± NADPH) for 2 min, the metabolic process was initiated by adding SJG-136. Reactions were terminated after 15–60 min incubation by immediate freezing on dry ice. Samples were prepared for analysis as described earlier.

Data analysis

Plasma concentration–time data were fitted to a two-compartment open model using the program WinNonlin Version 4.1 (Pharsight Corporation, Mountainview, CA, USA).

Results

Rat pharmacokinetics

The plasma profile of SJG-136 after a single bolus intravenous injection of a 15 μg/kg dose to Fisher CDF rats is illustrated in Fig. 2. The decline in SJG-136 plasma concentration was best fitted to a 2-compartment open model with distribution and elimination half-life values of 2.09 and 9.05 min, respectively. The peak plasma concentration and clearance values were 138 nM and 201 ml/min/m^2 (33.5 ml/min/kg), respectively (Table 1). The plasma profile of SJG-136 in Fisher CDF rats after bolus intravenous injection of 50 μg/kg is also illustrated in Fig. 2. Again, the decline in SJG-136 plasma concentration was best fitted to a 2-compartment open model with distribution and elimination half-life values of 1.38 and 8.34 min, respectively. The peak plasma concentration and clearance values were

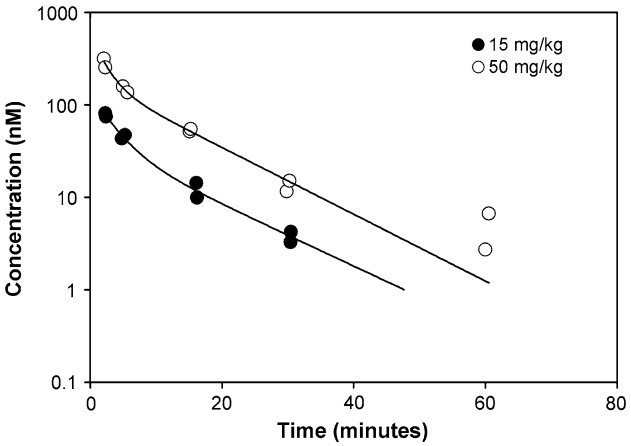

Fig. 2 SJG-136 plasma concentration–time profile following i.v. bolus administration of a 15-μg/kg (*closed circles*) and 50-μg/kg (*open circles*) SJG-136. *Solid line* Data fit to a 2-compartment open model

Table 1 SJG-136 Pharmacokinetics in male Fisher CDF Rats

	Estimate (±SE)	CV%	Estimate (±SE)	CV%
Dose (μg/kg)	15		50	
AUC (nM × min)	804 ± 32	4.1	2,996 ± 201	6.7
K_{10}-half-life (min)	4.05 ± 0.54	13.4	3.54 ± 1.00	28.4
α-half-life (min)	2.09 ± 0.59	28.1	1.38 ± 0.75	54.0
β-half-life (min)	9.05 ± 1.52	16.8	8.34 ± 1.61	19.2
V_D (ml/kg)	196 ± 29	14.7	154 ± 50	32.9
C_{max} (nM)	138 ± 20	14.7	586 ± 192	32.9
Cl (ml/min/kg)	33.5 ± 1.4	4.1	30.0 ± 2.0	6.7
V_{ss} (ml/kg)	313 ± 28	8.9	281 ± 44	15.6

586 nM and 180 ml/min/m^2 (30 ml/min/kg), respectively (Table 1). Acute toxicity was not observed with either SJG-136 dose.

SJG-136 plasma concentrations were measured on Day 1 and Day 5 30 min after treatment with 25 μg/kg/day for 5 consecutive days. SJG-136 was not toxic to rats treated with this dose and schedule. The mean plasma concentrations (n = 3) of 6.2 ± 3.2 nM on Day 1 and 4.7 ± 1.2 nM on Day 5 were in the concentration range expected based on the single-dose pharmacokinetic studies where the mean observed 30-min SJG-136 plasma concentration after a 50-μg/kg dose was 13.3 nM. SJG-136 did not accumulate in plasma after 5-days administration on this daily dose and schedule.

In vivo DNA damage by SJG-136

DNA damage (formation of single-strand breaks and cross-links) was measured in PBMCs from SJG-136-treated rats

using the Single Cell Gel Electrophoresis (Comet) assay. Using a method optimized for measuring DNA interstrand crosslinks and subsequently validated for use in the Phase I studies of this agent [12, 14], cross-linking measured as a percent decrease in tail moment was found in one of two rats treated with 15 μg/kg SJG-136 and both rats treated with 50 μg/kg (Fig. 3a). Substantial DNA cross-linking was detected in PBMCs 1 h after administration of 50 μg/kg SJG-136 and maintained throughout the 24-h observation period after drug administration. Under these conditions, no DNA single-strand breaks were observed in unirradiated samples at either dose. Using the alternative method, DNA single-strand breaks were detected in rat PBMCs after treatment with a single i.v. dose of 15 or 50 μg/kg SJG-136. Formation of DNA single-strand breaks was greater in PBMCs from rats treated with 50 μg/kg SJG-136; peak values were detected 4 h after drug administration; and returned to baseline 24 h following drug administration (Fig. 3b).

DNA damage was also assessed using the alternative method in PBMCs from rats treated with 25 μg/kg/day SJG-136 intravenously daily for 5 days. DNA cross-linking in PBMCs reached peak levels after 2 days' treatment with SJG-136 and remained elevated during the remainder of the 5-day treatment and for 3 days after the end of treatment (Fig. 3c). DNA single-strand breaks were detected in PBMCs 4 h after the first dose of SJG-136 (Fig. 3d). Further treatment with drug over the 5-day period was associated with a reduction in DNA single-strand breaks compared to day 1. Three days after the end of treatment a significant level of cross-linking was still observed, and DNA single-strand breaks were higher than at the end of the treatment period.

DNA damage was measured in rat PBMCs isolated from untreated rats and exposed in vitro to 150, 600, or 1200 nM SJG-136 for 1, 4, or 8 h using the Comet assay. Comet data for this experiment is illustrated in Fig. 4. Some DNA damage was observed in incubated PBMCs due to

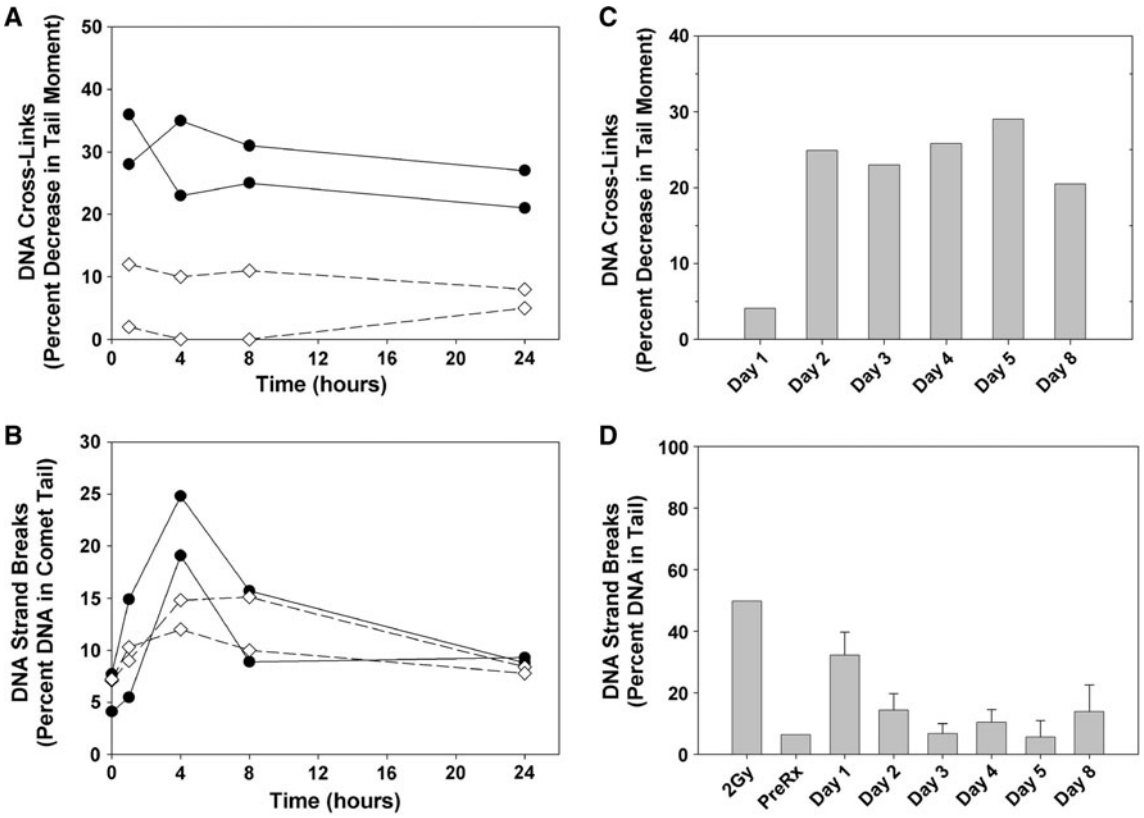

Fig. 3 DNA damage to rat lymphocyte DNA following i.v. administration of SJG-136. **a** DNA cross-linking produced by a single dose of 15 μg/kg (*open diamonds*) or 50 μg/kg (*closed circles*) SJG-136. **b** DNA strand breaks produced by a single dose of 15 μg/kg (*open diamonds*) or 50 μg/kg (*closed circles*) SJG-136. **c** DNA cross-linking produced during daily administration of 25 μg/kg SJG-136 to male Fisher CDF rats daily for 5 days. **d** DNA strand breaks produced during daily administration of 25 μg/kg SJG-136 to male Fisher CDF rats daily for 5 days. Each data point represents the mean value of four Comet measurements (two slides from each of two rats) where each Comet measurement was obtained from 25 images (pre-treatment) or 50 images (post-treatment) per slide. DNA cross-linking is expressed as percent decrease in moment of Comet tails after irradiation with 5 Gy. DNA strand breaks are expressed as percent of DNA in Comet tails without irradiation with strand breaks produced by 2-Gy irradiation shown as a positive control

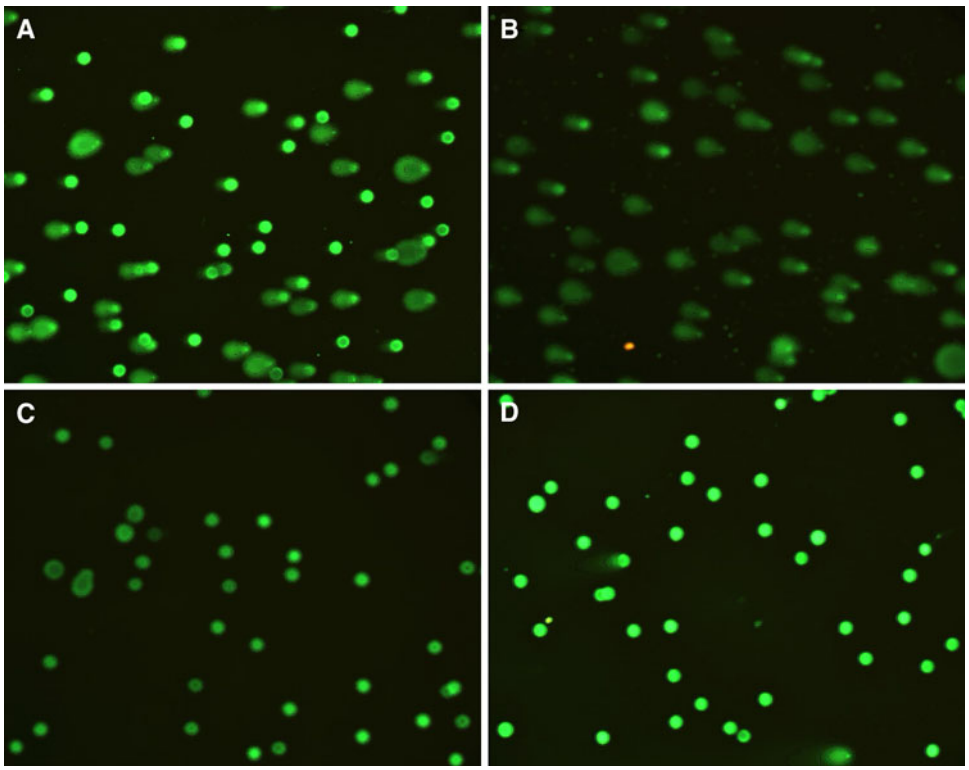

Fig. 4 Detection of DNA damage in PBMCs using the Comet assay following 8-h incubation in medium containing 0.1% DMSO in the presence or absence of SJG-136 **a** No treatment. **b** No treatment followed by exposure to 5 Gy of ionizing radiation. **c** Treatment with 150 nM SJG-136. **d** Treatment with 150 nM SJG-136 followed by 5 Gy of ionizing radition

mechanical damage caused by preparing cells for Comet analysis (Fig. 4a). Extensive DNA damage (Fig. 4b) was observed when cells were incubated with 5-Gy ionizing irradiation. As illustrated for 8-h exposure to 150 nM SJG-138, Comet tails were absent on images acquired before (Fig. 4c) and after (Fig. 4d) exposure to 5-Gy ionizing radiation. These data confirm extensive cross-linking in SJG-136-treated cells that prevented DNA damage due to both mechanical processes during sample preparation and treatment with 5-Gy ionizing radiation.

In vitro metabolism

SJG-136 was incubated with liver microsomes from untreated rats and rats treated with the CYP3A inducer dexamethasone, the CYP2B/CYP3A inducer phenobarbital or the CYP1A inducer 3-methylcholanthrene to investigate cytochrome P450-catalyzed oxidative metabolism. Less than 10% of the SJG-136 added to the microsomal reaction mixtures was consumed during the 120-min incubation in the absence of NADPH. In the presence of NADPH, greater than 90% of the added drug was metabolized after 30-min incubation with microsomes from phenobarbital- and dexamethasone-pretreated rats. Less than 35% of SJG-136 was consumed in reaction mixtures containing microsomes from untreated or 3-methylcholanthrene pretreated rats (Fig. 5a). When SJG-136 was co-incubated with CYP-selective chemical inhibitors (ketoconazole-CYP3A, erythromycin-CYP3A, quercitin-CYP3A and CYP1A, SKF-525A-non-specific and tolbutamide-CYP2C) and microsomes from dexamethasone- and phenobarbital-pretreated rats, the CYP3A inhibitors ketoconazole and erythromycin were the most potent CYP-selective inhibitors of SJG-136 metabolism (Fig. 5b). After preincubation of microsomal preparations from dexamethasone- or phenobarbital-pretreated rats with anti-rat CYP3A2 antiserum, SJG-136 metabolism was reduced by 40% and 100%, respectively (Fig. 5c). Finally, SJG-136 metabolism was detected in microsomal incubations containing recombinant rat CYP3A1 and CYP3A2, as well as human CYP3A4 (data not shown).

One anticipated metabolite resulting from the cytochrome P450-catalyzed oxidation of SJG-136 would be the PBD monomer (I) shown in Fig. 5d. This metabolite could be formed by α-hydroxylation of the C8/C8′-propyl linker followed by cleavage of the hemi-acetal to form I and a second PBD monomer II containing the C8-proprionaldehyde moiety. Consistent with this anticipated oxidation and cleavage of the C8/C8′-propyl linker, a product with m/z 259 corresponding to metabolite I along with its N10-C11-carbinolamine addition product at m/z 277 (not shown) were detected in microsomal reaction mixtures after incubation of SJG-136 in the presence of NADPH (Fig. 5e). No other metabolites were detected despite 90% disappearance of the parent drug. This was surprising, as formation of A-ring demethylated metabolites (e.g., Pathway B, Fig. 5d) might also be anticipated.

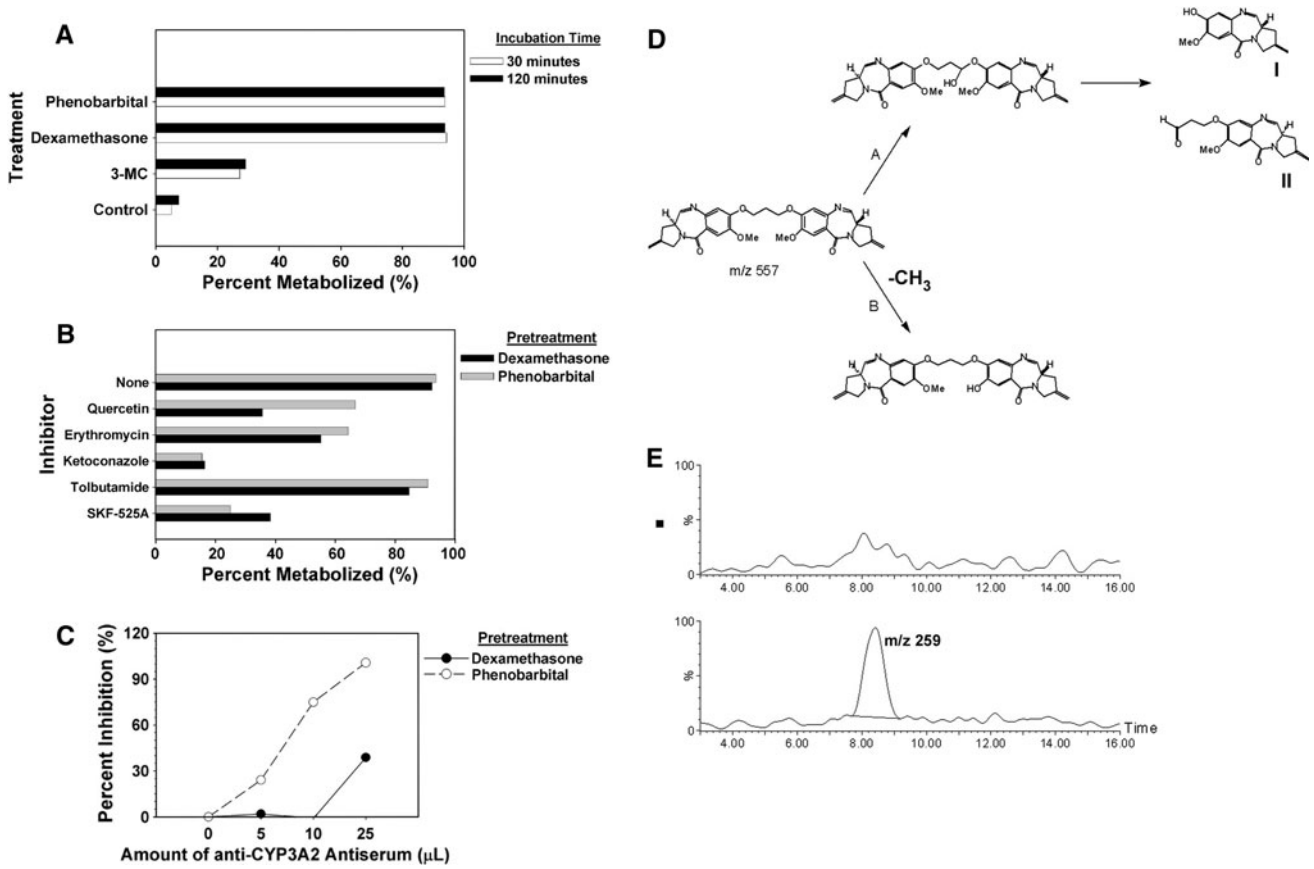

Fig. 5 Metabolism of SJG-136 by rat liver microsomes. **a** Metabolism by microsomal preparations from rats treated with enzyme-inducing drugs. **b** Inhibition of SJG-136 metabolism by cytochrome P450-selective chemical inhibitors. **c** Inhibition of SJG-136 metabolism in rat liver microsomes by anti-CYP3A2 antiserum. **d** Proposed pathway of SJG-136 oxidation by cytochromes P450. **e** Ion chromatograms of incubation extracts collected before initiating the reaction (*upper panel*) and after 15 min reaction (*lower panel*) of SJG-136 with rat CYP3A2. The m/z 259 ion produced by metabolite I was monitored. Phenobarbital, CYP2B/3A inducer; dexamethasone, CYP3A inducer; 3-MC, CYP1A inducer. Inhibitor selectivity—quercitin (CYP3A/CYP1A), erythromycin (CYP3A), ketoconazole (CYP3A), tolbutamide (CYP2C), and SKF-525A (non-specific)

Discussion

The sequence-selective, bifunctional DNA alkylating agent SJG-136 has potent in vitro cytotoxicity and in vivo antitumor activity attributed to DNA cross-linking after binding in the DNA minor groove [10]. Earlier pharmacokinetic studies of SJG-136 in mice [15] and dogs [19] reported peak plasma concentrations well above the GI_{50} values for sensitive cell lines in the NCI's in vitro 60 cell line screen, and also within the range of in vitro concentrations associated with DNA interstrand crosslinks in K562 human leukemia cells [8]. The purpose of this study was to describe the pharmacokinetics of SJG-136 in rats and to investigate damage to lymphocyte DNA as a potential in vivo pharmacodynamic marker for SJG-136 activity using the Single Cell Gel Electrophoresis (Comet) assay. In addition, we sought preliminary evidence of SJG-136 metabolism using rodent and human in vitro models in an attempt to predict the effect of metabolism on plasma clearance in clinical trials.

Peak plasma concentrations of SJG-136 in rats administered a 15-μg/kg dose were well above the in vitro GI_{50} values for sensitive cell lines in the NCI 60 cell line screen. However, rapid clearance reduced SJG-136 plasma concentrations to below these GI_{50} values within 60 min of drug administration. A 50-μg/kg dose of SJG-136 prolonged the period of time that SJG-136 plasma concentrations remained in the range associated with in vitro activity. Daily dosing with 25 μg/kg SJG-136 for 5 days maintained plasma drug concentration in the range associated with in vitro activity during that period.

CYP3A isoforms were found to be the predominant P450s involved in catalyzing in vitro metabolism of SJG-136 in rat liver microsomal preparations. This conclusion was based on preferential induction of metabolism by the CYP3A inducers phenobarbital and dexamethasone,

inhibition of metabolism by the CYP3A inhibitors quercitin, erythromycin and ketoconazole, and inhibition of metabolism by anti-CYP3A2 antiserum. Such results clearly predict a likely role for CYP3A isoforms in human metabolism [20, 21] and indicate that SJG-136 should be co-administered cautiously with drugs that are substrates, inhibitors, or inducers of CYP3A isoforms until the role of human CYP3A isoforms in the metabolism of SJG-136 is better understood.

As the in vitro antiproliferative activity of SJG-136 has been associated with interstrand cross-link formation between the N10-C11/N10′-Cll′ imine moieties in SJG-136 and the N2 groups of guanine bases situated on opposite DNA strands [10], we investigated the formation of DNA lesions in PBMCs following both in vitro and in vivo exposure to SJG-136. The Comet assay has been used to measure DNA lesions produced in PBMCs from patients treated with the DNA cross-linking agents ifosfamide [22], melphalan (ex vivo) [23] and a nitrogen mustard prodrug [24]. In earlier in vitro studies with SJG-136, DNA interstrand cross-links were detected in human leukemia K562 cells, and cross-linking was shown to increase with exposure to concentrations of up to 300 nM. Cross-links were also detected in tumor cells from mice implanted with xenograft tumors after administration of a dose of SJG-136 that caused significant growth delay when administered on a daily × 3 schedule [8]. We have also observed DNA damage attributable to interstrand cross-linking following in vitro exposure of rat PBMCs to SJG-136, consistent with those earlier studies (Fig. 4).

A single dose of SJG-136 yields peak plasma concentrations in rats, mice [15], and dogs [19] in a range of concentrations associated with in vitro DNA cross-linking and antiproliferative activity [8]. As illustrated in the studies reported here, for similar concentrations in rats, we have observed interstrand cross-links in PBMCs. The extent of cross-linking was dose and time dependent with the highest values detected 4 h after administration of a 50-μg/kg dose, and with values returning to baseline 24 h after a single dose. DNA cross-links accumulated during 5 consecutive days of dosing and persisted for at least three days after completion of daily dosing which may be indicative of delayed repair. In a recent phase I study of SJG-136, cross-links in PBMCs increased with systemic exposure and were still detected immediately before cycle 2 [14]. A similar accumulation of DNA lesions was observed during continuous infusion of ifosfamide for 3 and 4 days [22]. In the current study, dose- and time-dependent formation of DNA single-strand breaks were also detected in rat PBMCs following administration of SJG-136. In contrast to crosslinks, values returned to baseline within 24 h after a single-dose and lesions did not accumulate during 5 consecutive days of dosing.

It is noteworthy that in vitro exposure of rat PBMCs to SJG-136 produced DNA cross-links, but not DNA single-strand breaks, whereas PBMCs isolated from rats treated with SJG-136 contained both DNA cross-links and single-strand breaks. This could be due to CYP3A-catalyzed cleavage of the pyrrolobenzodiazepine dimer to monomeric metabolites as shown in Fig. 5. Once formed, these metabolites could produce mono-covalent DNA adducts leading to DNA strand breaks, as has been previously shown for the pyrrolobenzodiazepine monomer anthramycin [25]. Alternatively, it has been reported recently that in addition to interstrand cross-links, SJG-136 can form intrastrand cross-links and mono-covalent adducts [11]. Therefore, it is also possible that the extent and duration of exposure of PBMCs to SJG-136 in the in vivo experiments lead to a greater degree of mono-covalent adduct formation.

In conclusion, the pharmacokinetics of SJG-136 appear to be similar in mice, dogs, and rats. Plasma concentrations of SJG-136 associated with pharmacological activity and antitumor effect were achieved with doses that are both tolerable and active in these species. CYP3A isoforms appear to be the predominant P450s catalyzing SJG-136 metabolism, and we report the observation of metabolites I for the first time.

Acknowledgments Supported by National Cancer Institute contract N01-CM-07105. Supported by Cancer Research UK grant C2259/A9994 to JAH and the UCL Experimental Cancer Medicine Centre.

References

1. Gregson SJ, Howard PW, Jenkins TC, Kelland LR, Thurston DE (1999) Synthesis of a novel C2/C2′-*exo* unsaturated pyrrolobenzodiazepine cross-linking agent with remarkable DNA binding affinity and cytotoxicity. J Chem Soc Chem Commun 9:797–798
2. Gregson SJ, Howard PW, Gullick DR, Hamaguchi A, Corcoran KE, Brooks NA, Hartley JA, Jenkins TC, Patel S, Guille MJ, Thurston DE (2004) Linker length modulates DNA cross-linking reactivity and cytotoxic potency of C8/C8′ ether-linked C2-exo-unsaturated pyrrolo[2, 1-c][1, 4]benzodiazepine (PBD) dimers. J Med Chem 47(5):1161–1174
3. Thurston DE (1993) Advances in the study of pyrrolo[2, 1-c][1,4]benzodiazepine (PBD) antitumor antibiotics. In: Neidle S, Waring MJ (ed) Topics in molecular and structural biology: molecular aspects of anticancer drug-DNA interactions. The MacMillan Press Ltd., London, pp 54–88
4. Bose DS, Thompson AS, Ching J (1992) Rational design of a highly efficient irreversible DNA interstrand coss-linking agent based on the pyrrolobenzodiazepine ring system. J Am Chem Soc 114:4939–4941
5. Smellie M, Kelland LR, Thurston DE, Souhami RL, Hartley JA (1994) Cellular pharmacology of novel C8-linked anthramycin-based sequence-selective DNA minor groove cross-linking agents. Br J Cancer 70(1):48–53
6. Walton MI, Goddard P, Kelland LR, Thurston DE, Harrap KR (1996) Preclinical pharmacology and antitumour activity of the

novel sequence-selective DNA minor-groove cross-linking agent DSB-120. Cancer Chemother Pharmacol 38(5):431–438
7. Alley MC, Hollingshead MG, Pacula-Cox CM, Waud WR, Hartley JA, Howard PW, Gregson SJ, Thurston DE, Sausville EA (2004) SJG-136 (NSC 694501), a novel rationally designed DNA minor groove interstrand cross-linking agent with potent and broad spectrum antitumor activity: part 2: efficacy evaluations. Cancer Res 64(18):6700–6706
8. Hartley JA, Spanswick VJ, Brooks N, Clingen PH, McHugh PJ, Hochhauser D, Pedley RB, Kelland LR, Alley MC, Schultz R, Hollingshead MG, Schweikart KM, Tomaszewski JE, Sausville EA, Gregson SJ, Howard PW, Thurston DE (2004) SJG-136 (NSC 694501), a novel rationally designed DNA minor groove interstrand cross-linking agent with potent and broad spectrum antitumor activity: part 1: cellular pharmacology, in vitro and initial in vivo antitumor activity. Cancer Res 64(18):6693–6699
9. Pepper CJ, Hambly RM, Fegan CD, Delavault P, Thurston DE (2004) The novel sequence-specific DNA cross-linking agent SJG-136 (NSC 694501) has potent and selective in vitro cytotoxicity in human B-cell chronic lymphocytic leukemia cells with evidence of a p53-independent mechanism of cell kill. Cancer Res 64(18):6750–6755
10. Smellie M, Bose DS, Thompson AS, Jenkins TC, Hartley JA, Thurston DE (2003) Sequence-selective recognition of duplex DNA through covalent interstrand cross-linking: kinetic and molecular modeling studies with pyrrolobenzodiazepine dimers. Biochem 42(27):8232–8239
11. Rahman KM, Thompson AS, James CH, Narayanaswamy M, Thurston DE (2009) The pyrrolobenzodiazepine dimer SJG-136 forms sequence-dependent intrastrand DNA cross-links and monoalkylated adducts in addition to interstrand cross-links. J Am Chem Soc 131(38):13756–13766
12. Hochhauser D, Meyer T, Spanswick VJ, Wu J, Clingen PH, Loadman P, Cobb M, Gumbrell L, Begent RH, Hartley JA, Jodrell D (2009) Phase I study of sequence-selective minor groove DNA binding agent SJG-136 in patients with advanced solid tumors. Clin Cancer Res 15(6):2140–2147
13. Janjigian YY, Lee W, Kris MG, Miller VA, Krug LM, Azzoli CG, Senturk E, Wade Calcutt M, Rizvi NA (2010) A phase I trial of SJG-136 (NSC#694501) in advanced solid tumors. Cancer Chemother Pharmacol 65(5):833–838
14. Puzanov I, Lee W, Berlin JD, Calcutt MW, Hachey DL, Vermeulen WL, Spanswick VJ, Hartley JA, Chen AP, Rothenburg ML (2008) Final results of phase I and pharmacokinetic trial of SJG136 administered on a daily x 3 schedule. J Clin Oncol 26 (suppl):2504
15. Wilkinson GP, Taylor JP, Shnyder S, Cooper P, Howard PW, Thurston DE, Jenkins TC, Loadman PM (2004) Preliminary pharmacokinetic and bioanalytical studies of SJG-136 (NSC 694501), a sequence-selective pyrrolobenzodiazepine dimer DNA-cross-linking agent. Invest New Drugs 22(3):231–240
16. Spanswick VJ, Hartley JM, Ward TH, Hartley JA (1999) Measurement of drug-indcued DNA interstrand crosslinking using the single cell gel electrophoresis (Comet) assay. In: Brown B (ed) Cytotoxic drug resistance mechanisms, methods in molecular medcine. Humana Press, USA, pp 143–154
17. Olive PL, Banath JP, Durand RE (1990) Heterogeneity in radiation-induced DNA damage and repair in tumor and normal cells measured using the "comet" assay. Radiat Res 122(1):86–94
18. Helma C, Uhl M (2000) A public domain image-analysis program for the single-cell gel-electrophoresis (comet) assay. Mutat Res 466(1):9–15
19. Buhrow SA, Reid JM, Jia L, McGovern RM, Covey JM, Kobs DJ, Grossi IM, Ames MM (2006) LC-MS/MS assay and dog pharmacokinetics of the dimeric pyrrolobenzodiazepine SJG-136 (NSC 694501). J Chromatogr B Analyt Technol Biomed Life Sci 840(1):56–62
20. Guengerich FP (1999) Cytochrome P-450 3A4: regulation and role in drug metabolism. Annu Rev Pharmacol Toxicol 39:1–17
21. Soucek P, Gut I (1992) Cytochromes P-450 in rats: structures, functions, properties and relevant human forms. Xenobiotica 22(1):83–103
22. Hartley JM, Spanswick VJ, Gander M, Giacomini G, Whelan J, Souhami RL, Hartley JA (1999) Measurement of DNA cross-linking in patients on ifosfamide therapy using the single cell gel electrophoresis (comet) assay. Clin Cancer Res 5(3):507–512
23. Spanswick VJ, Craddock C, Sekhar M, Mahendra P, Shankaranarayana P, Hughes RG, Hochhauser D, Hartley JA (2002) Repair of DNA interstrand crosslinks as a mechanism of clinical resistance to melphalan in multiple myeloma. Blood 100(1): 224–229
24. Webley SD, Francis RJ, Pedley RB, Sharma SK, Begent RH, Hartley JA, Hochhauser D (2001) Measurement of the critical DNA lesions produced by antibody-directed enzyme prodrug therapy (ADEPT) in vitro, in vivo and in clinical material. Br J Cancer 84(12):1671–1676
25. Petrusek RL, Uhlenhopp EL, Duteau N, Hurley LH (1982) Reaction of anthramycin with DNA. Biological consequences of DNA damage in normal and xeroderma pigmentosum cell. J Biol Chem 257(11):6207–6216